



Published in final edited form as:

Cell Stem Cell. 2014 May 1; 14(5): 673–688. doi:10.1016/j.stem.2014.03.002.

Epigenomic profiling of young and aged HSCs reveals concerted changes during aging that reinforce self-renewal

Deqiang Sun^{1,2,9}, Min Luo^{1,9}, Mira Jeong^{1,9}, Benjamin Rodriguez², Zheng Xia², Rebecca Hannah³, Hui Wang⁴, Thuc Le⁵, Kym F. Faull⁵, Rui Chen⁴, Hongcang Gu⁷, Christoph Bock^{7,8}, Alex Meissner⁷, Berthold Göttgens³, Gretchen J. Darlington^{6,10}, Wei Li^{2,10,*}, and Margaret A. Goodell^{1,2,10,*}

¹Stem Cells and Regenerative Medicine Center, Department of Pediatrics and Molecular & Human Genetics, Baylor College of Medicine, One Baylor Plaza, Houston, TX 77030 USA

²Dan L Duncan Cancer Center and Department of Molecular and Cellular Biology, Baylor College of Medicine, Houston, Texas 77030, USA

³Department of Hematology, Cambridge Institute for Medical Research and Wellcome Trust and MRC Cambridge Stem Cell Institute, Cambridge University, Hills Road, CB2 0XY Cambridge, UK

⁴Human Genome Sequencing Center, Baylor College of Medicine, Houston, Texas 77030, USA

⁵Pasarow Mass Spectrometry Laboratory, Department of Psychiatry and Biobehavioral Sciences and the Semel Institute for Neuroscience and Human Behavior, David Geffen School of Medicine, University of California Los Angeles, Los Angeles, CA 90095, USA

⁶Huffington Center on Aging, Baylor College of Medicine, Houston, Texas 77030, USA

⁷Broad Institute of MIT and Harvard, Cambridge, MA, 02142, USA, Department of Stem Cell and Regenerative Biology, Harvard University, Cambridge, MA

SUMMARY

To investigate the cell-intrinsic aging mechanisms that erode the function of somatic stem cells during aging, we have conducted a comprehensive integrated genomic analysis of young and aged cells. We profiled the transcriptome, DNA methylome, and histone modifications of young and old murine hematopoietic stem cells (HSCs). Transcriptome analysis indicated reduced TGF β signaling and perturbation of genes involved in HSC proliferation and differentiation. Aged HSCs exhibited broader H3K4me3 peaks across HSC identity and self-renewal genes, and showed

© 2014 Il Press. All rights reserved.

*Corresponding authors: WL1@bcm.edu and goodell@bcm.edu.

⁸Now at CeMM Research Center for Molecular Medicine, Lazarettgasse 14, AKH BT 25.3 Vienna, Austria

⁹Co-first authors

¹⁰Co-senior authors

SUPPLEMENTARY INFORMATION

Supplemental information includes Extended Experimental Procedures, 7 tables and figures. Data sets are accessible at GEO (GSE47819) (www.ncbi.nlm.nih.gov/geo/). Data and genome browser tracks can also be found at: <http://www.aginghscepigenome.us>

Publisher's Disclaimer: This is a PDF file of an unedited manuscript that has been accepted for publication. As a service to our customers we are providing this early version of the manuscript. The manuscript will undergo copyediting, typesetting, and review of the resulting proof before it is published in its final citable form. Please note that during the production process errors may be discovered which could affect the content, and all legal disclaimers that apply to the journal pertain.

increased DNA methylation at transcription factor binding sites associated with differentiation-promoting genes combined with a reduction at genes associated with HSC maintenance. Together these changes reinforce HSC self-renewal and diminish differentiation, paralleling phenotypic HSC aging behavior. Ribosomal biogenesis emerged as a particular target of aging, with increased transcription of ribosomal protein and RNA genes, and hypomethylation of rRNA genes. This dataset will serve as a reference for future epigenomic analysis of stem cell aging.

INTRODUCTION

The function of the hematopoietic system declines with age, manifested by a decreased adaptive immune response, and an increased incidence of myeloproliferative diseases, autoimmune and inflammatory disorders (Linton and Dorshkind, 2004; Ramos-Casals et al., 2003). While some extrinsic cellular factors such as an inflammatory microenvironment promote aging (Ergen et al., 2012; Villeda et al., 2011), these impact the hematopoietic stem cells (HSCs), causing cell-intrinsic changes that affect the generation of a balanced supply of differentiated blood lineages.

Multiple lines of investigation have established that with age, phenotypically-defined mouse and human HSCs increase in number while lymphoid cell production is diminished leading to a myeloid-dominant hematopoietic system (Chambers et al., 2007b; de Haan and Van Zant, 1999; Morrison et al., 1996; Rossi et al., 2005). The myeloid dominance is caused partly by a shift in the clonal composition of the HSC compartment (Beerman et al., 2010; Challen et al., 2010; Cho et al., 2008), but also reflects diminished differentiation capacity of individual HSCs (Dykstra et al., 2011).

Mechanisms proposed to account for the age-related loss of HSC function include telomere shortening, accumulation of nuclear and mitochondrial DNA damage (Wang et al., 2012), and coordinated variation in gene expression. Analysis of young and old HSCs revealed that genes associated with inflammation and stress response were up-regulated, and genes involved in DNA repair and chromatin silencing were down-regulated with HSC aging (Chambers et al., 2007b; Rossi et al., 2005). These earlier studies were conducted on HSC populations that proved to be heterogeneous and therefore represented a mix of cellular phenotypes. Here, we examined highly purified HSCs and tested the concept that loss of epigenetic regulation of gene expression in aged HSCs could explain the constellation of aging phenotypes. We completed genome-wide comparisons of the transcriptome (RNA-Seq), histone-modification (ChIP-Seq) and DNA methylation between young and old purified murine bone marrow HSCs. This report presents an integrated analysis of these genomic properties, reveals potential mechanisms that contribute to HSC aging, and offers the first comprehensive reference epigenome of any somatic stem cell type. Finally, it reveals similarities with some common hallmarks of aging (Lopez-Otin et al., 2013) previously noted in model organisms such as *C. elegans* and *D. melanogaster* but not yet examined in mammals. systems.

RESULTS

Alterations in Gene Expression with Age

Because previous analyses of gene expression changes with age utilized HSC populations that are now known to be heterogeneous with regard to lymphoid vs. myeloid production proficiency, we utilized the most primitive HSCs with the highest long-term self-renewal potential, considered myeloid-biased (or lymphoid deficient). HSCs throughout this study were purified as SP-KSL-CD150⁺ (see methods), as these are found in both young and aged mice and have high phenotypic homogeneity and functional activity (Challen et al., 2010; Mayle et al., 2012). High-throughput sequencing of poly A⁺ RNA (RNA-Seq) from purified 4 month- (4mo), and 24 month-old (24mo) HSCs was performed. With biological duplicates, more than 200 million reads in total for each age of HSC were obtained, offering high sensitivity to detect gene expression differences in young and aged HSCs.

Comparison of the young and old HSC transcriptomes revealed that 1,337 genes were up-regulated, and 1,297 genes were down-regulated with HSC aging (FDR<0.05, Table S1). Aging HSC hallmark genes *Clusterin (Clu)* and *P-selectin (Selp)* (Chambers et al., 2007b) were markedly upregulated, although their expression was also detectable in young HSCs, demonstrating the sensitivity of RNA sequencing.

Gene ontology (GO) analyses indicated that genes up-regulated in 24mo HSCs are highly enriched in categories related to Cell Adhesion, Cell Proliferation and the Ribosome, while down-regulated genes are enriched in DNA Base Excision Repair, DNA replication and Cell Cycle (Figure 1A). GSEA analysis with the Molecular Signature Database as well as several customized HSC, myeloid and lymphoid gene sets (“fingerprint” genes) (Chambers et al., 2007a) (Table S2) revealed that HSC-specific genes as a group were upregulated in old HSC, in agreement with their increased phenotypic stem cell characteristics. Cell cycle, DNA replication and glutamate signaling were also differentially expressed gene sets.

The Aging HSC Transcriptome Suggests Reduced TGF- β signaling

We next sought to infer the key regulators responsible for transcriptional changes in aging HSCs. We performed a functional enrichment analysis based on expected cause-effect relationships between transcriptional regulators and their targets in the Ingenuity Pathway Analysis database. The most highly represented upstream regulator was growth factor TGF- β 1, accounting for ~ 19% of differential gene expression in young versus old HSC (p-value = 1.96E-33) (Table S3). Compared to all genes affected by age, TGF- β -regulated genes were five times more likely to be altered in expression than expected by chance (p-value = 3.53E-20). As a group, 63% (136 of 217) of TGF- β 1-downstream genes were associated with a diversity of biological functions supporting hematopoiesis (n = 83, p-value = 4.56E-24 – 1.29E-09) and/or are corroborated by earlier microarray-based studies of HSC aging (n = 86) (Table S3).

Depending on the context, TGF- β factors exert pleiotropic and sometimes opposing cellular effects. If TGF- β 1 signaling were inhibited, we would expect key intermediary transcription factors to be similarly affected. To test this, we constructed a network of cooperating regulators that are connected downstream of TGF- β 1 by one edge. This analysis identified

Smad3, Sp1, and Egr1 and predicted that they were inhibited during HSC aging (Figure S1, Table S3). Indeed, expression of *Egr1*, a regulator of HSC homeostasis (Min et al., 2008), is significantly reduced with aging. Additional groups of genes normally activated by TGF- β are of interest. Seven collagen and 3 metalloproteinase (Mmp) genes, implicated in HSC-niche interactions, were down regulated. In addition, expression of TGF- β -regulated genes involved in HSC development, such as *Nr4a1*, *Cepba*, *Jun* and *Junb* was reduced. Reduction of several of these targets could contribute to myeloid differentiation bias.

Of genes up-regulated with aging, one notable class was ribosomal protein genes, including a majority of those encoding both the large (*Rpl*) and small (*Rps*) subunits (Figure 1B), but not mitochondrial ribosomal protein groups (*Mrpl* and *Mrps*) (confirmed by exon arrays (Figure S2A)). Up-regulation of genes involved in protein synthesis has been previously noted with aging. Indeed, inhibition of ribosomal proteins or their regulators has been shown to extend life span in yeast and worms (Kaeberlein et al., 2005; Syntichaki et al., 2007). However, changes in the expression of ribosomal protein genes have not been previously reported in mammalian stem cells.

Expression of key epigenetic regulators decreases with age

As we hypothesized that epigenetic regulation plays a role in HSC aging, we examined expression of epigenetic modifiers (Figure 1C). *Ezh1* showed increased expression, consistent with previous findings (Hidalgo et al., 2012). In contrast, *Ezh2* and the Polycomb Group (PcG) complex member *Cbx2* decreased in old HSCs. In addition, expression of histone kinase genes *Aurka* and *Aurkb*, putative *Ezh2* partners or targets (Kamminga et al., 2006), also decreased with age.

Genes encoding DNA methyltransferases (Dnmts) as a group decreased during aging (FDR=0.02) (Figure 1C, Table S2). Concomitantly, genes encoding Tet1 and Tet3 DNA demethylation proteins were also decreased. While their functions are unknown, *Tet2* mutation leads to expansion of hematopoietic progenitors and increased stem cell self-renewal (Ko et al., 2011; Li et al., 2011; Moran-Crusio et al., 2011; Quivoron et al., 2011) and *TET2* is recurrently mutated in MDS and AML patients (Delhommeau et al., 2009; Langemeijer et al., 2009). Consistent with reduction of Tet gene expression, quantitative mass spectrometry revealed reduced 5-hydroxymethylcytosine (5hmC) with age (Figure 1D).

Repetitive elements are epigenetically repressed, so we examined whether they were dysregulated with aging. Strikingly, the RNA-Seq data revealed marked changes in the expression of multiple repetitive elements with age, including 168 LTR elements, 113 LINE elements, 67 SINE elements, and 32 other repeat elements. 68%~76% of these exhibited increased expression. This increased repetitive element expression may result from aberrant epigenetic repression, and could contribute to increased genome instability (Figure 1E). Anomalous repetitive element expression has been associated with ES cells (Xie et al., 2013) but not with aging. Examination of the genes near the dysregulated LTR, LINE, and SINE elements revealed 194, 127, and 72 genes, respectively. Functional enrichment by GREAT indicated LINE and SINE-associated genes were enriched for these involved in hematological diseases, such as *Cdc42*, *Flt3* and *Lmo2* (Table S4).

Alterations in transcript isoform expression

RNA-seq also revealed age-associated changes in promoter usage and pre-mRNA abundance. We identified 118 genes that showed switched promoter usage during aging (Table S4). One example is *Runx1t1*, a locus translocated to *RUNX1* in some types of AML. The full-length *Runx1t1* is expressed in old HSCs, with the short isoform in young (Figure S2B). Another example is *Nfkbiz*, with expression of the short isoform decreased with aging (Figure S2C).

We previously noted that HSCs contain significant incompletely spliced mRNA that is reduced when HSCs are activated (Venezia et al., 2004). Global pre-mRNA quantification here confirmed a full 13% of reads within Refseq introns in young HSCs, which decreased with age (Figure S2D). Nearly 300 genes showed age-associated alteration of pre-mRNA abundance. Of the 184 genes with decreased pre-mRNA abundance, many were classified in Ribosome, Immunoglobulin domain and Extracellular Region categories by GO analysis (for example, *Ctla2a* and ribosome protein *Rpl13* Figure S2E), while the 96 genes with increased pre-mRNA were enriched in Zinc Finger-encoding genes (Figure S2F). The decreased pre-mRNA with age may be associated with increased translation.

HSC-specific chromatin features

To examine epigenetic alterations, we profiled the principal regulatory chromatin marks in HSCs, specifically H3K4me3, H3K27me3 and H3K36me3 marks in young (4mo) and old (24mo) HSCs using ChIP-seq. Because these global analyses have never been performed on such highly purified HSCs, we first describe our general observations.

In young HSCs, 10,263 Refseq genes had clear H3K4me3 associated peaks. Clustering of the signal around the transcription start sites (TSS) show that the H3K4me3 peaks can be classified into three distinct clusters (Figure 2A). Cluster 1 overlaps with 2373 genes and shows high intensity and wide coverage (mean 3200pb) into the gene body. Cluster 2 (2225 genes) and Cluster 3 (5665 genes) have similar intensity and coverage lengths (~2000bp) but cluster 2 has more coverage upstream of the TSS. The remaining Refseq genes have little or no discernible H3K4me3 peak (cluster 4).

For the repressive H3K27me3 mark in young HSCs, we identified 3768 peaks present in the promoter region defined as the TSS \pm 1 kb. Unsupervised clustering showed the majority with a sharp peak over the TSS (cluster 2; distinct from the H3K4 clusters). A small subset showed high levels spread over most of the coding region (cluster 1, Figure 2B). For H3K36me3, the signals are depleted at the TSS and increase from the TSS to the TTS (Figure 2C). As in other cell types, this mark was strongly correlated with gene expression and enriched in the gene body. H3K36me3 and H3K27me3 signals were generally mutually exclusive (Figure S3A).

Genes with both activating H3K4me3 and repressive H3K27me3 were first identified in embryonic stem cells (ESC) as so-called “bivalent” genes, thought to represent poised master regulators (Bernstein et al., 2006). Here, 2267 out of 3768 H3K27me3-enriched genes in HSC also contain H3K4me3 (Figure 2D), similar to the proportions in ESC (although we cannot confirm that the marks are on the same allele). These genes were

enriched for development, transcriptional regulation and RNA metabolism GO categories (Figure 2E), consistent with previous observations (Weishaupt et al., 2010). Many transcription factors important for hematopoietic differentiation, such as *Cebpa*, *Ebf-1*, *Pax5*, and *Gata3*, appeared bivalent. Notably, one third of the bivalent HSC genes are glycoproteins involved in signaling pathways such as Wnt, Hedgehog, BMP and TGF- β . Their expression was generally low (Figure S3B).

Next, we attempted to identify potential HSC regulators based on histone modifications. We compared ESC H3K4me3 and H3K27me3 binding sites (Bernstein et al., 2006) with those from HSCs as well as differentiated B cells and Granulocytes (Gr) (Figure 2F). We selected genes that were developmental regulators (bivalent in ESC), were activated in HSCs (H3K4me3 only), but were repressed upon HSC differentiation (regained H3K27me3 in differentiated B cells and Granulocytes), to identify 255 genes (Figure 2G, Table S5). These are enriched for transcription factors and pathways in cancer (Figure S3C). Significantly, 20% of them overlap with HSC fingerprint genes (Chambers et al., 2007a), including *Cd34*, *Gata2* and *Meis1*, whose functions in HSCs have been demonstrated, showing that histone profiles can independently predict key HSC regulators.

Aging-associated changes in histone marks

We next examined aging-associated histone mark changes. While most shifts were moderate there were some unique features. Old HSCs exhibited a 6.3% increase in the number of H3K4me3 peaks, many of which were considerably broader with age; more than half of all H3K4me3 peaks expanded and less than 10% shrank (Figure 3A). The expansion of H3K4me3 coverage was greatest for peaks already broad in young HSCs; for peaks longer than 3kb in young HSCs, there are 69% and 7% of lengthening and shortening events respectively (Figure S3D). Peak expansion was particularly striking at genes associated with HSC identity (Figure S3E).

More H3K4me3 coverage in old HSCs suggested that some previously unexpressed transcripts are activated. The levels of H3K4me3 were significantly increased on 267, and decreased on 73 promoters in the old HSC (Figure 3B). We observed a strong positive correlation between altered H3K4me3 signal and gene expression changes (Figure 3C). Increased H3K4me3 was observed for the most up-regulated genes, such as *Selp*, *Nupr1*, *Sdpr*, *Plscr2* and *Slamf1*, and genes in the *HoxB* cluster (Figure S3F). In addition, increased H3K4me3 was associated with altered promoter usage, for example at the *oxidation resistance 1 (Oxr1)* gene, revealing a new unannotated promoter (Figure 3D).

PcG-mediated epigenetic alteration is considered a driving force behind many age-related changes and is often dysregulated in human malignancies. We observed similar H3K27me3 peak counts with age, but increased length of coverage by 29% from 203 to 261 Mb, and the average signal intensity at TSS increased by ~50%, similar to quiescent satellite cells (Liu et al., 2013). H3K27me3 binding increased at 402 and decreased at 124 promoters (Figure 3E). Notably, at the *Flt3* locus, H3K27me3 was increased and expression decreased (Figure S3G), consistent with the diminished lymphoid differentiation potential of aged HSCs.

One well-known target of the PcG family during aging is *Cdkn2a* (encoding p16^{INK4a}), which showed progressive loss of H3K27me₃-associated repression and increased expression with aging in neural stem cells (NSC) (Molofsky et al., 2006). Increased *Cdkn2a* is considered a primary indicator of cellular senescence in virtually all tissues in mice and humans (Lopez-Otin et al., 2013). However, HSCs represent a stark exception; our results show that p16^{INK4a} is a bivalent gene effectively repressed by H3K27me₃ in both 4mo and 24mo HSC, and its expression remains undetectable at either age (Figure S3H). These data argue against the notion that loss of function of HSCs with age is due to acquisition of a senescent state linked to p16.

Considering the global changes of H3K4me₃ and H3K27me₃ with HSC aging, we reexamined the bivalent domains. The results indicated that 335 bivalent domains disappear in old HSCs, while 1245 emerge, largely due to gain of both H3K4me₃ and H3K27me₃, or H3K27me₃ only (Figure 3F). The genes that lose H3K27me₃ are enriched for the category of membrane protein, while the genes that gain H3K27me₃ are enriched for glycoprotein and cell adhesion (Figure S3I and Table S5).

HSC specific methylome

We also examined DNA methylation changes with aging. Global CpG hypomethylation associated with aging has been observed in many tissues and is thought to contribute to genome instability and the risk of neoplastic transformation (Maegawa et al., 2010). Here, we used whole genome bisulfite sequencing (WGBS) and generated 1,494 million (4mo HSCs), and 1,493 million (24mo HSCs) reads; about 82.6% and 84.3%, respectively, were aligned to the reference genome (mm9). Of all cytosines present in the reference genome, about 93% of Cs and 99% of CGs were covered in both datasets, with an average coverage of 46-fold (4mo) and 50-fold (24mo).

Globally, the HSC methylome exhibited the DNA methylation patterns in line with those observed in other mammalian cells (Stadler et al., 2011). Low DNA methylation was found in CpG islands (CGIs) and promoters, and high methylation in gene bodies and repetitive elements (Figure 4A and Figure S4A–C). Bivalent domains showed the lowest DNA methylation (5%) (Figure S4D), consistent with the inverse correlation of DNA methylation and H3K4me₃ (Meissner et al., 2008). In contrast, H3K36me₃-enriched regions are associated with the highest DNA methylation (94%), possibly attributed to Dnmt3a and H3K36me₃ interaction (Dhayalan et al., 2010). Interestingly, the CGI methylation is diverse and dependent on the genomic or epigenomic context (Figure S4E).

We also compared the HSC and ESC (Stadler et al., 2011) methylomes. 5% of CGIs show differential methylation between these two stem cell types with 689 CGIs hypermethylated in HSC and 130 CGIs hypomethylated (Figure 4B). We further identified differentially methylated regions (DMRs) between HSC and ESC as a region of at least 100 bp in length wherein consecutive CpGs show the same hyper- or hypo-methylation state. Analysis showed striking enrichment of “positive transcription factor (TF) regulation” for hypo-DMR genes and “negative TF regulation” for hyper-DMR genes. Of 10 well-known hematopoietic transcription factors (Wilson et al., 2010), all had hypomethylated promoter regions and their target binding sites were also hypomethylated. For example, the *Runx1* promoter is

methylated in ESC, unmethylated in HSC (Figure 4C), and its binding sites showed a strong bias toward hypomethylation in HSCs (Figure 4D). Taken together, the general methylation pattern in different genomic regions is conserved in HSC, but methylation of cell-type-specific TFs and their binding sites is unique to HSCs.

Aging-dependent DNA methylation and interaction with histone modifications

In contrast to the age-associated hypomethylation observed in somatic cells, HSCs showed methylation increasing with age from 83.5% to 84.6% in old HSCs, consistent with previous studies focused on CGI (Beerman et al., 2013). We observed a total of 448,166 differentially methylated CpGs (DMCs) ($\pm 20\%$ difference), of which 38.5% were hypomethylated (hypo-DMCs) and 61.5% were hypermethylated (hyper-DMCs). For different genomic features (Table S6), a slightly greater DNA methylation increase was observed for the gene body, LINEs and SINEs, while CGIs and promoters showed balanced increases and decreases (Figure 5A). DNA encoding for ribosome RNA (rDNA) was a hotspot for hypo-DMCs (Figure 5B). CpGs with an intermediate methylation ratio were more susceptible to alterations than fully methylated or unmethylated CpGs (Figure S5A). We also found that increased H3K4me3 strongly correlated with hypo-methylation, H3K27me3 regions are hot spots for both hypo- and hyper-DMCs (Table S6), and decreased H3K36me3 correlated with hypo-DMCs (Figure 5C).

To identify the genes or pathways subject to DNA methylation alterations, we screened the methylome for DMRs. We identified 4,828 hypo- and 4,523 hyper-DMRs between 4mo and 24mo HSC, that were associated with 2,253 and 2,071 genes respectively (Table S7). Calculating the Pearson correlation between the methylation and gene expression changes, we discovered that DMRs between the TSS and the 1 kb immediately downstream showed the highest correlation with gene expression (-0.312), followed by the DMRs in the promoters lacking CpG islands (-0.250) (Figure S5B). Hypo-DMR-associated genes are enriched for pathways in cancer, and include *Bcl2*, *Ptk2*, *Rb1*, *Mll3*, *Runx1*, *Flt3l*, *Myc*, *Igf1*, *Igf1r*, *NFkb2*, *Tgfb3* and *Tgfb2*. In contrast, both hypo-DMR and hyper-DMR genes are enriched in old HSCs for cell adhesion and actin cytoskeleton, such as *Arpc1a*, *Ablim2*, *Cadm1*, *Cdh1*, *Col2a1*, *CD34*, *CD40* and *CD86* (Figure S5C and Table S7)

DNA hypermethylation on polycomb-targeted genes is a hallmark of cancer and aging. Here we compared H3K27me3 marked genes in both young and old HSCs with the DMR gene list. We found that 40% of hyper-DMR genes contain H3K27me3 marks, while 25% of hypo-DMR genes contained H3K27me3, confirming that polycomb targeted genes are hotspots for aging-related DNA methylation (Figure 5D). One example is *Nr4a2*, a regulator of HSC quiescence (Sirin et al., 2010), that gained methylation on the H3K27me3-marked domain with age, correlated with suppression of the short isoform (Figure S5D). To examine whether an epigenetic signature alone might identify potential biomarkers of aging, we identified ~50 genes that showed concomitant DNA methylation and histone H3K4me3 differences during HSC aging (Figure 5E). These loci showed a particularly strong inverse correlation between their age-related decrease in DNA methylation and their increased H3K4me3 (64%) (Figure S5E), but not all of them showed increased gene expression

(Figure S5F). These results indicate that the epigenetic state may be used to predict aging independent of gene expression.

Aging-associated DNA methylation interferes with the transcriptional network

Previous DNA methylation studies showed that hypomethylated regions (HMR) are usually associated with cell-specific regulatory regions or TF binding sites (Hodges et al., 2011; Stadler et al., 2011; Ziller et al., 2013). To determine whether the methylation states in such regulatory regions change with HSC aging, we examined the methylation ratio in the binding sites of five TFs associated with HSC pluripotency, including *Scl*, *Erg*, *Gata2*, *Runx1* and *Ldb1* (Wilson et al., 2010). While basal methylation levels for these TF binding sites in HSC are low (Figure S6A), methylation at *Gata2* and *Ldb1* binding sites are further reduced with age (Figure S6B). This led us to further test whether aberrant DNA methylation disrupts the HSC transcriptional networks more broadly. We compiled genome-wide binding sites of more than 150 TFs found in a variety of blood lineages (>10) and compared them with DMRs identified in young and old HSCs. The results revealed that hypo-DMRs are significantly enriched for *Ring1b*, *Scl*, *Gata1*, *Ldb1* and *Runx1* binding sites in old HSCs, but not for *Rad21* binding sites, which served as a negative control (Figure 6A). Combinatorial interactions of *Scl/Lyl1/Gata2/Runx1/Lmo2/Fli1/Erg* have been suggested to form a central transcription network that regulates HSC pluripotency (Wilson et al., 2010). Hypomethylation of the binding sites for some of these factors or related family members may therefore play a role in reinforcing the self-renewal program in HSCs. In parallel, hyper-DMRs are highly enriched for *Pu.1*, *Fli1*, *Gfi1* and *Erg* binding sites in old HSCs (Figure 6B). Among them, binding sites of *Pu.1*, which promotes HSC differentiation, showed hypermethylation with the highest statistical significance (Figure 6C). As mutation or deletion of *PU.1* is leukemogenic (Cook et al., 2004), hypermethylation of its binding sites may increase the risk for myeloid leukemia.

We also examined changes with age in methylation of canyons, which comprise around 1,100 large regions with low methylation enriched for genes involved in transcriptional regulation (Jeong et al., 2014). Hypomethylation is 25 – 28% more frequent at inner edges of Canyons whereas hypermethylation is 25% more frequent at outside edges (Figure 6D). Furthermore, canyons with more hypomethylated DMCs are associated with greater H3K4me3 coverage, while canyons with more hypermethylated DMCs show a distinct shift in H3K27me3 occupancy characterized by both a substantial decline in partial coverage (spanning < 25 % of canyon length) and an increase in broader H3K27me3 coverage (spanning > 90% of canyon length) (Figure 6E). This is similar to the behavior of canyons after *Dnmt3a* KO (Jeong et al., 2014).

All of these findings suggest that DNA methylation is a critical layer of epigenetic regulation controlling HSC aging, and underscore some of the similarities between the epigenetic changes with aging and those in *Dnmt3a* KO HSCs.

Methylation alterations identify HSC regulators and age-associated phenotypes

To determine whether changes in DNA methylation were likely to affect HSC function, we compared DMR genes with HSC, myeloid and lymphoid fingerprint genes. Strikingly, of

HSC fingerprint genes, 70% showed hypomethylation (Table S7), which correlated with their increased expression (-0.45) (Figure 7A and Figure S7A). Hypermethylation and decreased expression was also observed on a subset of HSC fingerprint genes. To test whether their decreased expression might explain HSC aging phenotypes, we selected the imprinted gene *Slc22a3*, encoding a solute carrier family member (Grundemann et al., 1998), for further characterization (Figure 7B). To examine its function, we transduced progenitors from young mice with a retroviral miRNA knockdown construct. After 2 days of culture, transduced cells were sorted for qRT-PCR to confirm a knockdown efficiency of about 60% (Figure 7C), mimicking its expression change in old HSCs. While transplantation showed knockdown of *Slc22a3* did not affect engraftment, there was a greater proportion of myeloid cells generated from *Slc22a3*-knockdown HSCs (Figure 7D). Thus, decreased expression of *Slc22a3* may contribute to the myeloid-biased differentiation of old HSCs.

Myelodysplastic syndrome (MDS) is a hematologic disorder that increases dramatically with age. We considered whether some of the changes associated with normal HSC aging were associated with MDS. We examined 66 MDS-related genes as defined by IPA. Twenty-one contained a DMR (p value= $1E-16$), and their methylation changes were generally inversely-correlated with gene expression changes (Figure 7E). Five contain both hypo- and hyper-DMRs, such as *Hspa1a* (Figure S7B). Notably, the gene for splicing factor *Sf3b1* contains a hyper-DMR at its TSS region and shows decreased expression. Somatic mutation of this gene has been found in 20% of MDS patients (Papaemmanuil et al., 2011). The disordered methylation on those MDS-associated genes may contribute to the development of this disease.

DISCUSSION

In summary, we present a comprehensive report of the transcriptome and epigenetic signatures, including DNA methylation and three histone modifications, of highly purified young and old HSCs, which can serve as a resource for both normal and aging adult stem cell studies. The epigenetic alterations are closely correlated with the phenotypic and functional changes that have been documented for HSC, namely the increased HSC self-renewal, diminished differentiation potential, and biased ratio of myeloid vs. lymphoid differentiation. While not directly pathological, the epigenetic changes we observe clearly provide a cellular environment conducive to age-related pathologies, such as MDS and leukemia, as outlined below.

Age-related changes suggest reduced TGF- β signaling

Our analyses of the transcriptome of young and old HSCs strikingly implicate TGF- β as likely to be among the most significant contributors to the functional age-related declines that occur in this stem cell type with age. While decreased TGF- β signaling has been implicated in aging of cardiac and neural tissue (Blaney Davidson et al., 2005; Loffredo et al., 2013), here we observed genes involved in specific signaling modules that are likely mediating the altered TGF- β response. In the context of the HSC, we are inferring responses to stimuli that are likely initiated by the niche based on the large number of dysregulated TGF- β genes.

For each step of the TGF- β 1 signaling pathway, there are a number of differentially expressed genes in aging HSC. For example, genes involved in ligand activation or bioavailability were decreased, such as matrix metalloproteases mmp-2, mmp-9 (Yu and Stamenkovic, 2000). We also observed decreased expression of the gene for Smad6, which interferes with phosphorylation of Smad2 (Imamura et al., 1997) and Smad cofactors p300, Crebbp, and Atf3. Given these data, as well as the long-standing evidence for a role in TGF- β signaling on HSC function (Fan et al., 2002; Jacobsen et al., 1995), further study of the role of TGF- β signaling in HSC aging is warranted.

Significance of the altered ribosomal gene transcription

In the transcriptome, epigenome and methylome data, we found that genes included in the GO category Ribosome were a prominent target of aging. In particular, the decreased ribosomal protein gene pre-mRNA levels suggest more efficient splicing and possibly translation. Even though aged HSCs are not more in cycle than young HSCs (Chambers et al., 2007b; Rossi et al., 2005), they may be more activated. Intriguingly, defects in ribosome biogenesis have been linked to bone marrow failure syndromes associated with a risk of developing malignancies, such as Diamond-Blackfan anemia (Narla and Ebert, 2010). In addition, ribosomal biogenesis has repeatedly been linked to aging in model organisms (Curran and Ruvkun, 2007; Grewal, 2009; Hamilton et al., 2005; Pan et al., 2007) but not yet in mammals. Our data suggest that a reexamination of the role of the ribosome in mammalian stem cell aging should be undertaken.

Consistency of HSC aging with general organismal aging

Our observations regarding the increase in H3K4me3 peaks and the increased length of many of the peaks is striking in the context of recent observations in *C. elegans* where mutation of genes involved in H3K4 methylation increased longevity (Greer et al., 2010). This phenomenon was dependent on a histone demethylase (Greer et al., 2011), indicating that sustained H3K4-methylation activity promotes aging. Although we do not identify loss or gain of H3K4 methyltransferases, the accumulation of H3K4me3 with age, particularly on genes in which H3K4-trimethylation is already broad, likely contributes to the dysfunction of HSCs in the older animals. Notably, the genes associated with increased H3K4me3 breadth are specifically those associated with stem cell self-renewal and loss of differentiation capacity. Thus, the increase of this activating mark on these particular genes may be linked to the functional changes that occur in aged HSCs. We reanalyzed data from a recent study on aging of muscle satellite cells (Liu et al., 2013) and found that H3K4me3 length also increased by about 5% with age (not shown). It will be important to extend these observations of H3K4me3 to other aging systems, and identify the critical targets and mechanisms

Relationship between normal HSC aging and Myeloid Malignancies

MDS and myeloid leukemia are increasingly common with age. While heterogeneous, both of these diseases are marked by impeded differentiation and a shift toward myeloid output. Our data suggest that even in the absence of discernable mutations, aging HSCs acquire a host of changes that are consistent with a predisposition to MDS and myeloid malignancies.

For example, we see that expression of genes for key the epigenetic regulators *Dnmt3a* and *Ezh2* (both of which are found mutated in MDS and AML) are slightly but significantly down-regulated with age. We also see HSC-specific genes such as *Gata2* and *Hmga2* are hypomethylated and up-regulated, and that binding sites of transcription factors associated with differentiation, such as Pu.1, tend to become hypermethylated, whereas sites associated with factors involved in stem cell function (e.g. *Scl*) tend to be hypomethylated. Finally, we showed that the edges of DNA methylation canyons are highly dynamic in a manner concordant with loss of *Dnmt3a* function (Jeong et al., 2014), mutation of which is associated with hematologic malignancies (Ley et al., 2010; Yan et al., 2011). While our data cannot distinguish cause and effect with regard to these epigenetic changes with age, together, they point to a stem cell state in which self-renewal is reinforced and differentiation is impeded, a cellular milieu likely to be conducive to transformation events.

Abating the effects of age

By using whole genome analyses, we showed that concerted epigenetic changes may contribute to decreased differentiation and increased stem cell self renewal. These data also show the impact of epigenetic changes on aging is consistent, suggesting the possibility that some of the effects might be abated. Although aging is often regarded as an inexorable and irreversible process, emerging views suggests that the aging clock can be experimentally manipulated. Taken together, the findings here may allow the development of novel approaches to modulate HSC function.

EXPERIMENTAL PROCEDURES

Animals

C57BL/6 male mice were purchased from the National Institute for Aging (NIA) and maintained at the Baylor College of Medicine Animal Care Facility under IUCAC and institutional guidelines. None of the animals exhibited overt signs of pathology when sacrificed. We chose 24 months because this time point presages significant mortality increase and health-span decline.

Hematopoietic Stem Cell Purification and Flow Cytometry

HSCs were purified from bone marrow of mice either 4 or 24 months of age. For all experiments, HSCs were purified as Hoechst side population (SP) – KLS (c-kit⁺, lineage⁻, Sca1⁺) and CD150⁺ cells (also see extended experimental procedures). Bone marrow cells were stained for 90 minutes with Hoechst, magnetically enriched for cells with c-expression, stained with additional antibodies, then subjected to flow cytometric cell sorting. Purity was typically 95%.

RNA-sequencing

Batches of approximately 70,000 HSCs, 1 million B cell and Gr cells were FACS sorted. RNA was isolated with the RNeasy Micro kit (Qiagen, Valencia, CA). Paired end libraries were generated by using Illumina TruSeq RNA sample preparation kit. Illumina HiSeq was used for sequencing with a paired-end sequencing length of 100bp. For analysis, the alignment was performed by RUM which first tries to map reads to genome and

transcriptome by Bowtie, and then the reads unmapped to genome are handed to Blat for additional mapping. The information from the three mappings is merged into one mapping. The multiply mapped reads are then discarded. The gene annotations used for transcriptome alignment include standard known-gene models (see extended methods). Differential expression was performed using DESeq. We used DAVID to examine these differentially expressed genes for functional enrichment in GO terms, KEGG Pathways, and SP_PIR_KEYWORDS. The unbiased Gene Set Enrichment Analysis was performed using GSAA-Seq (<http://gsaa.unc.edu>), which ranks all genes by DESeq differential test p-values and examines enrichment of all gene sets in the Molecular Signatures Database (MSigDB) and several manually created hematopoiesis fingerprint gene sets.

ChIP-sequencing (ChIP-seq)

Chromatin Immunoprecipitation (ChIP) was performed with 50,000 to 100,000 HSCs, B-cells, and Granulocytes (see extended methods). ChIPed DNA was made into sequencing libraries using ThruPLEX-FD (Rubicon, Ann Arbor, MI). Sequencing was performed on an Illumina HiSeq 2000 and mapped to the mm9 mouse genome. and peaks were identified by model-based analysis of ChIP-seq data (MACS). The young and old samples were sequenced multiple times. The reads are mapped to mouse genome mm9 using SOAP2 by allowing at most 2 mismatches for 50bp long short reads and at most 4 mismatches for 100bp long short reads. Only uniquely mapped reads were retained. The reads from each biological replicate are fed as a treatment file into the MACS program to find the peaks.

Whole-genome bisulfite sequencing (WGBS)

300ng genomic DNA was isolated from HSCs and fragmented using a Covaris sonication system (Covaris S2). Libraries were constructed using Illumina TruSeq DNA kit, ligated, and bisulfite-treated using the EpiTect Kit (Qiagen, Valencia, CA). After determining the optimized PCR cycle number for each samples, a large scale PCR reaction (100 µl) was performed (Gu et al., 2011). PCR products were sequenced with Illumina HiSeq sequencing systems. The WGBS data analyses were based on the program MOABS: MOdel based Analysis of Bisulfite Sequencing (Sun et al. <http://code.google.com/p/moabs/>).

Statistical and Bioinformatic Analysis

See Extended Experimental Procedures.

Supplementary Material

Refer to Web version on PubMed Central for supplementary material.

Acknowledgments

This work is dedicated to Estela Medrano. We thank Julio Hernandez for mouse management and Chris Threeton for flow cytometry. This work was supported by grants AG036562, AG288652, CA126752, DK092883, CA125123, DK084259, DK056338, AI07495, AG000183, the Ellison Medical Foundation, CPRIT grant RP110028 and the Samuel Waxman foundation; to W.L.: HG007538, CPRIT RP110471, and DOD W81XWH-10-1-0501. Support for TL came from T32 MH 19384-14, T32-HD007032, and the Eugene V. Cota-Robles Fellowship. DS, ML and MJ designed and performed experiments; DS, BR, ML, MJ, TL, KFF, RC, GJD, MAG, WL, RH, HC, CB, AM and BG analyzed the data; and DS, ML, BR, MJ, TL, KFF, BG, MAG, WL, and GJD wrote and edited the manuscript.

References

- Beerman I, Bhattacharya D, Zandi S, Sigvardsson M, Weissman IL, Bryder D, Rossi DJ. Functionally distinct hematopoietic stem cells modulate hematopoietic lineage potential during aging by a mechanism of clonal expansion. *Proceedings of the National Academy of Sciences of the United States of America*. 2010; 107:5465–5470. [PubMed: 20304793]
- Beerman I, Bock C, Garrison BS, Smith ZD, Gu H, Meissner A, Rossi DJ. Proliferation-Dependent Alterations of the DNA Methylation Landscape Underlie Hematopoietic Stem Cell Aging. *Cell Stem Cell*. 2013
- Bernstein BE, Mikkelsen TS, Xie X, Kamal M, Huebert DJ, Cuff J, Fry B, Meissner A, Wernig M, Plath K, et al. A bivalent chromatin structure marks key developmental genes in embryonic stem cells. *Cell*. 2006; 125:315–326. [PubMed: 16630819]
- Blaney Davidson EN, Scharstuhl A, Vitters EL, van der Kraan PM, van den Berg WB. Reduced transforming growth factor-beta signaling in cartilage of old mice: role in impaired repair capacity. *Arthritis Res Ther*. 2005; 7:R1338–1347. [PubMed: 16277687]
- Challen GA, Boles NC, Chambers SM, Goodell MA. Distinct hematopoietic stem cell subtypes are differentially regulated by TGF-beta1. *Cell Stem Cell*. 2010; 6:265–278. [PubMed: 20207229]
- Chambers SM, Boles NC, Lin KY, Tierney MP, Bowman TV, Bradfute SB, Chen AJ, Merchant AA, Sirin O, Weksberg DC, et al. Hematopoietic fingerprints: an expression database of stem cells and their progeny. *Cell Stem Cell*. 2007a; 1:578–591. [PubMed: 18371395]
- Chambers SM, Shaw CA, Gatzka C, Fisk CJ, Donehower LA, Goodell MA. Aging hematopoietic stem cells decline in function and exhibit epigenetic dysregulation. *PLoS Biol*. 2007b; 5:e201. [PubMed: 17676974]
- Cho RH, Sieburg HB, Muller-Sieburg CE. A new mechanism for the aging of hematopoietic stem cells: aging changes the clonal composition of the stem cell compartment but not individual stem cells. *Blood*. 2008; 111:5553–5561. [PubMed: 18413859]
- Cook WD, McCaw BJ, Herring C, John DL, Foote SJ, Nutt SL, Adams JM. PU.1 is a suppressor of myeloid leukemia, inactivated in mice by gene deletion and mutation of its DNA binding domain. *Blood*. 2004; 104:3437–3444. [PubMed: 15304397]
- Curran SP, Ruvkun G. Lifespan regulation by evolutionarily conserved genes essential for viability. *PLoS Genet*. 2007; 3:e56. [PubMed: 17411345]
- de Haan G, Van Zant G. Dynamic changes in mouse hematopoietic stem cell numbers during aging. *Blood*. 1999; 93:3294–3301. [PubMed: 10233881]
- Delhommeau F, Dupont S, Della Valle V, James C, Trannoy S, Masse A, Kosmider O, Le Couedic JP, Robert F, Alberdi A, et al. Mutation in TET2 in myeloid cancers. *N Engl J Med*. 2009; 360:2289–2301. [PubMed: 19474426]
- Dhayalan A, Rajavelu A, Rathert P, Tamas R, Jurkowska RZ, Ragozin S, Jeltsch A. The Dnmt3a PWWP domain reads histone 3 lysine 36 trimethylation and guides DNA methylation. *J Biol Chem*. 2010; 285:26114–26120. [PubMed: 20547484]
- Dykstra B, Olthof S, Schreuder J, Ritsema M, de Haan G. Clonal analysis reveals multiple functional defects of aged murine hematopoietic stem cells. *J Exp Med*. 2011; 208:2691–2703. [PubMed: 22110168]
- Ergen AV, Boles NC, Goodell MA. Rantes/Ccl5 influences hematopoietic stem cell subtypes and causes myeloid skewing. *Blood*. 2012; 119:2500–2509. [PubMed: 22289892]
- Fan X, Valdimarsdottir G, Larsson J, Brun A, Magnusson M, Jacobsen SE, ten Dijke P, Karlsson S. Transient disruption of autocrine TGF-beta signaling leads to enhanced survival and proliferation potential in single primitive human hemopoietic progenitor cells. *J Immunol*. 2002; 168:755–762. [PubMed: 11777969]
- Greer EL, Maures TJ, Hauswirth AG, Green EM, Leeman DS, Maro GS, Han S, Banko MR, Gozani O, Brunet A. Members of the H3K4 trimethylation complex regulate lifespan in a germline-dependent manner in *C. elegans*. *Nature*. 2010; 466:383–387. [PubMed: 20555324]
- Greer EL, Maures TJ, Ucar D, Hauswirth AG, Mancini E, Lim JP, Benayoun BA, Shi Y, Brunet A. Transgenerational epigenetic inheritance of longevity in *Caenorhabditis elegans*. *Nature*. 2011; 479:365–371. [PubMed: 22012258]

- Grewal SS. Insulin/TOR signaling in growth and homeostasis: a view from the fly world. *Int J Biochem Cell Biol.* 2009; 41:1006–1010. [PubMed: 18992839]
- Grundemann D, Schechinger B, Rappold GA, Schomig E. Molecular identification of the corticosterone-sensitive extraneuronal catecholamine transporter. *Nat Neurosci.* 1998; 1:349–351. [PubMed: 10196521]
- Gu H, Smith ZD, Bock C, Boyle P, Gnirke A, Meissner A. Preparation of reduced representation bisulfite sequencing libraries for genome-scale DNA methylation profiling. *Nat Protoc.* 2011; 6:468–481. [PubMed: 21412275]
- Hamilton B, Dong Y, Shindo M, Liu W, Odell I, Ruvkun G, Lee SS. A systematic RNAi screen for longevity genes in *C. elegans*. *Genes Dev.* 2005; 19:1544–1555. [PubMed: 15998808]
- Hidalgo I, Herrera-Merchan A, Ligos JM, Carramolino L, Nunez J, Martinez F, Dominguez O, Torres M, Gonzalez S. Ezh1 Is Required for Hematopoietic Stem Cell Maintenance and Prevents Senescence-like Cell Cycle Arrest. *Cell Stem Cell.* 2012; 11:649–662. [PubMed: 23122289]
- Hodges E, Molaro A, Dos Santos CO, Thekkat P, Song Q, Uren PJ, Park J, Butler J, Raffii S, McCombie WR, et al. Directional DNA methylation changes and complex intermediate states accompany lineage specificity in the adult hematopoietic compartment. *Mol Cell.* 2011; 44:17–28. [PubMed: 21924933]
- Imamura T, Takase M, Nishihara A, Oeda E, Hanai J, Kawabata M, Miyazono K. Smad6 inhibits signalling by the TGF-beta superfamily. *Nature.* 1997; 389:622–626. [PubMed: 9335505]
- Jacobsen FW, Stokke T, Jacobsen SE. Transforming growth factor-beta potently inhibits the viability-promoting activity of stem cell factor and other cytokines and induces apoptosis of primitive murine hematopoietic progenitor cells. *Blood.* 1995; 86:2957–2966. [PubMed: 7579388]
- Jeong M, Sun D, Luo M, Huang Y, Challen GA, Rodriguez B, Zhang X, Chavez L, Wang H, Hannah R, et al. Large conserved domains of low DNA methylation maintained by Dnmt3a. *Nat Genet.* 2014; 46:17–23. [PubMed: 24270360]
- Kaerberlein M, Powers RW 3rd, Steffen KK, Westman EA, Hu D, Dang N, Kerr EO, Kirkland KT, Fields S, Kennedy BK. Regulation of yeast replicative life span by TOR and Sch9 in response to nutrients. *Science.* 2005; 310:1193–1196. [PubMed: 16293764]
- Kamminga LM, Bystrykh LV, de Boer A, Houwer S, Douma J, Weersing E, Dontje B, de Haan G. The Polycomb group gene Ezh2 prevents hematopoietic stem cell exhaustion. *Blood.* 2006; 107:2170–2179. [PubMed: 16293602]
- Ko M, Bandukwala HS, An J, Lamperti ED, Thompson EC, Hastie R, Tsangaratou A, Rajewsky K, Korolov SB, Rao A. Ten-Eleven-Translocation 2 (TET2) negatively regulates homeostasis and differentiation of hematopoietic stem cells in mice. *Proceedings of the National Academy of Sciences of the United States of America.* 2011; 108:14566–14571. [PubMed: 21873190]
- Langemeijer SM, Kuiper RP, Berends M, Knops R, Aslanyan MG, Massop M, Stevens-Linders E, van Hoogen P, van Kessel AG, Raymakers RA, et al. Acquired mutations in TET2 are common in myelodysplastic syndromes. *Nat Genet.* 2009; 41:838–842. [PubMed: 19483684]
- Ley TJ, Ding L, Walter MJ, McLellan MD, Lamprecht T, Larson DE, Kandoth C, Payton JE, Baty J, Welch J, et al. DNMT3A mutations in acute myeloid leukemia. *N Engl J Med.* 2010; 363:2424–2433. [PubMed: 21067377]
- Li Z, Cai X, Cai CL, Wang J, Zhang W, Petersen BE, Yang FC, Xu M. Deletion of Tet2 in mice leads to dysregulated hematopoietic stem cells and subsequent development of myeloid malignancies. *Blood.* 2011; 118:4509–4518. [PubMed: 21803851]
- Linton PJ, Dorshkind K. Age-related changes in lymphocyte development and function. *Nat Immunol.* 2004; 5:133–139. [PubMed: 14749784]
- Liu L, Cheung TH, Charville GW, Hurgo BM, Leavitt T, Shih J, Brunet A, Rando TA. Chromatin modifications as determinants of muscle stem cell quiescence and chronological aging. *Cell Rep.* 2013; 4:189–204. [PubMed: 23810552]
- Loffredo FS, Steinhauser ML, Jay SM, Gannon J, Pancoast JR, Yalamanchi P, Sinha M, Dall'Osso C, Khong D, Shadrach JL, et al. Growth differentiation factor 11 is a circulating factor that reverses age-related cardiac hypertrophy. *Cell.* 2013; 153:828–839. [PubMed: 23663781]
- Lopez-Otin C, Blasco MA, Partridge L, Serrano M, Kroemer G. The hallmarks of aging. *Cell.* 2013; 153:1194–1217. [PubMed: 23746838]

- Maegawa S, Hinkal G, Kim HS, Shen L, Zhang L, Zhang J, Zhang N, Liang S, Donehower LA, Issa JP. Widespread and tissue specific age-related DNA methylation changes in mice. *Genome Res.* 2010; 20:332–340. [PubMed: 20107151]
- Mayle A, Luo M, Jeong M, Goodell MA. Flow cytometry analysis of murine hematopoietic stem cells. *Cytometry Part A: the journal of the International Society for Analytical Cytology.* 2012
- Meissner A, Mikkelsen TS, Gu H, Wernig M, Hanna J, Sivachenko A, Zhang X, Bernstein BE, Nusbaum C, Jaffe DB, et al. Genome-scale DNA methylation maps of pluripotent and differentiated cells. *Nature.* 2008; 454:766–770. [PubMed: 18600261]
- Min IM, Pietramaggiore G, Kim FS, Passegue E, Stevenson KE, Wagers AJ. The transcription factor EGR1 controls both the proliferation and localization of hematopoietic stem cells. *Cell Stem Cell.* 2008; 2:380–391. [PubMed: 18397757]
- Molofsky AV, Slutsky SG, Joseph NM, He S, Pardal R, Krishnamurthy J, Sharpless NE, Morrison SJ. Increasing p16INK4a expression decreases forebrain progenitors and neurogenesis during ageing. *Nature.* 2006; 443:448–452. [PubMed: 16957738]
- Moran-Crusio K, Reavie L, Shih A, Abdel-Wahab O, Ndiaye-Lobry D, Lobry C, Figueroa ME, Vasanthakumar A, Patel J, Zhao X, et al. Tet2 loss leads to increased hematopoietic stem cell self-renewal and myeloid transformation. *Cancer Cell.* 2011; 20:11–24. [PubMed: 21723200]
- Morrison SJ, Wandycz AM, Akashi K, Globerson A, Weissman IL. The aging of hematopoietic stem cells. *Nature medicine.* 1996; 2:1011–1016.
- Narla A, Ebert BL. Ribosomopathies: human disorders of ribosome dysfunction. *Blood.* 2010; 115:3196–3205. [PubMed: 20194897]
- Pan KZ, Palter JE, Rogers AN, Olsen A, Chen D, Lithgow GJ, Kapahi P. Inhibition of mRNA translation extends lifespan in *Caenorhabditis elegans*. *Aging Cell.* 2007; 6:111–119. [PubMed: 17266680]
- Papaemmanuil E, Cazzola M, Boultonwood J, Malcovati L, Vyas P, Bowen D, Pellagatti A, Wainscoat JS, Hellstrom-Lindberg E, Gambacorti-Passerini C, et al. Somatic SF3B1 mutation in myelodysplasia with ring sideroblasts. *N Engl J Med.* 2011; 365:1384–1395. [PubMed: 21995386]
- Quivoron C, Couronne L, Della Valle V, Lopez CK, Plo I, Wagner-Ballon O, Do Cruzeiro M, Delhommeau F, Arnulf B, Stern MH, et al. TET2 inactivation results in pleiotropic hematopoietic abnormalities in mouse and is a recurrent event during human lymphomagenesis. *Cancer Cell.* 2011; 20:25–38. [PubMed: 21723201]
- Ramos-Casals M, Garcia-Carrasco M, Brito MP, Lopez-Soto A, Font J. Autoimmunity and geriatrics: clinical significance of autoimmune manifestations in the elderly. *Lupus.* 2003; 12:341–355. [PubMed: 12765297]
- Rossi DJ, Bryder D, Zahn JM, Ahlenius H, Sonu R, Wagers AJ, Weissman IL. Cell intrinsic alterations underlie hematopoietic stem cell aging. *Proceedings of the National Academy of Sciences of the United States of America.* 2005; 102:9194–9199. [PubMed: 15967997]
- Sirin O, Lukov GL, Mao R, Conneely OM, Goodell MA. The orphan nuclear receptor Nurr1 restricts the proliferation of haematopoietic stem cells. *Nat Cell Biol.* 2010; 12:1213–1219. [PubMed: 21076412]
- Stadler MB, Murr R, Burger L, Ivanek R, Lienert F, Scholer A, van Nimwegen E, Wirbelauer C, Oakeley EJ, Gaidatzis D, et al. DNA-binding factors shape the mouse methylome at distal regulatory regions. *Nature.* 2011; 480:490–495. [PubMed: 22170606]
- Syntichaki P, Troulinaki K, Tavernarakis N. eIF4E function in somatic cells modulates ageing in *Caenorhabditis elegans*. *Nature.* 2007; 445:922–926. [PubMed: 17277769]
- Venezia TA, Merchant AA, Ramos CA, Whitehouse NL, Young AS, Shaw CA, Goodell MA. Molecular signatures of proliferation and quiescence in hematopoietic stem cells. *PLoS Biol.* 2004; 2:e301. [PubMed: 15459755]
- Villeda SA, Luo J, Mosher KI, Zou B, Britschgi M, Bieri G, Stan TM, Fainberg N, Ding Z, Eggel A, et al. The ageing systemic milieu negatively regulates neurogenesis and cognitive function. *Nature.* 2011; 477:90–94. [PubMed: 21886162]
- Wang J, Sun Q, Morita Y, Jiang H, Gross A, Lechel A, Hildner K, Guachalla LM, Gompf A, Hartmann D, et al. A differentiation checkpoint limits hematopoietic stem cell self-renewal in response to DNA damage. *Cell.* 2012; 148:1001–1014. [PubMed: 22385964]

- Weishaupt H, Sigvardsson M, Attema JL. Epigenetic chromatin states uniquely define the developmental plasticity of murine hematopoietic stem cells. *Blood*. 2010; 115:247–256. [PubMed: 19887676]
- Wilson NK, Foster SD, Wang X, Knezevic K, Schutte J, Kaimakis P, Chilarska PM, Kinston S, Ouwehand WH, Dzierzak E, et al. Combinatorial transcriptional control in blood stem/progenitor cells: genome-wide analysis of ten major transcriptional regulators. *Cell Stem Cell*. 2010; 7:532–544. [PubMed: 20887958]
- Xie W, Schultz MD, Lister R, Hou Z, Rajagopal N, Ray P, Whitaker JW, Tian S, Hawkins RD, Leung D, et al. Epigenomic analysis of multilineage differentiation of human embryonic stem cells. *Cell*. 2013; 153:1134–1148. [PubMed: 23664764]
- Yan XJ, Xu J, Gu ZH, Pan CM, Lu G, Shen Y, Shi JY, Zhu YM, Tang L, Zhang XW, et al. Exome sequencing identifies somatic mutations of DNA methyltransferase gene DNMT3A in acute monocytic leukemia. *Nat Genet*. 2011; 43:309–315. [PubMed: 21399634]
- Yu Q, Stamenkovic I. Cell surface-localized matrix metalloproteinase-9 proteolytically activates TGF-beta and promotes tumor invasion and angiogenesis. *Genes Dev*. 2000; 14:163–176. [PubMed: 10652271]
- Ziller MJ, Gu H, Muller F, Donaghey J, Tsai LT, Kohlbacher O, De Jager PL, Rosen ED, Bennett DA, Bernstein BE, et al. Charting a dynamic DNA methylation landscape of the human genome. *Nature*. 2013; 500:477–481. [PubMed: 23925113]

HIGHLIGHTS

- Epigenome and transcriptome mapping of young and aged hematopoietic stem cells
- TGF- β -signaling, ribosome biogenesis and H3K4me3 marking perturbed
- Epigenetic dysregulation reinforces self-renewal and encumbers differentiation
- HSC aging parallels organismal aging and predisposition to malignancy

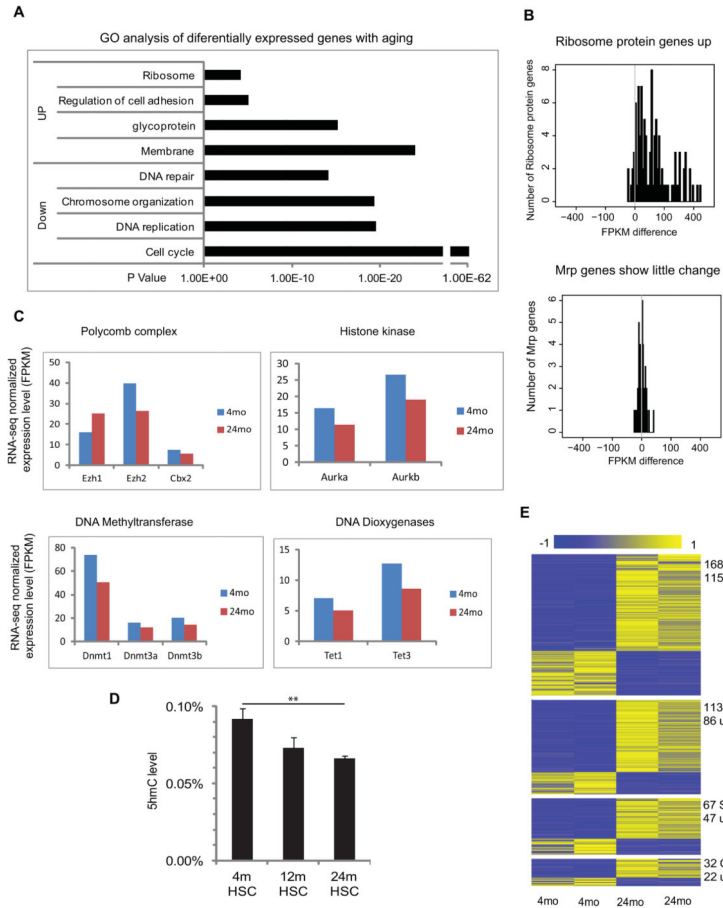


Figure 1. Transcriptome alterations with HSC aging

(A) Gene ontology enrichment analysis for 2140 differentially expressed genes with HSC aging; X-axis shows the P value.

(B) The distribution of expression changes for ribosomal protein genes during HSC aging, where the x-axis value is FPKM difference between Old and Young HSC.

(C) Average FPKM value of genes encoding epigenetic modifiers in young and old HSCs.

(D) HPLC-mass-spectrometry measurements of 5-hydroxy methylcytosine (5hmC) levels as a proportion of the total cytosine in purified HSCs from 4mo, 12mo and 24mo old mice (n=7). ** P< 0.01. Error bars represent Mean \pm SEM.

(E) Differential expression of repetitive elements during HSC. Each row represents a repeat location in the genome. Blue denotes low and yellow high expression (log₂ reads number). See also Figures S1, and S2

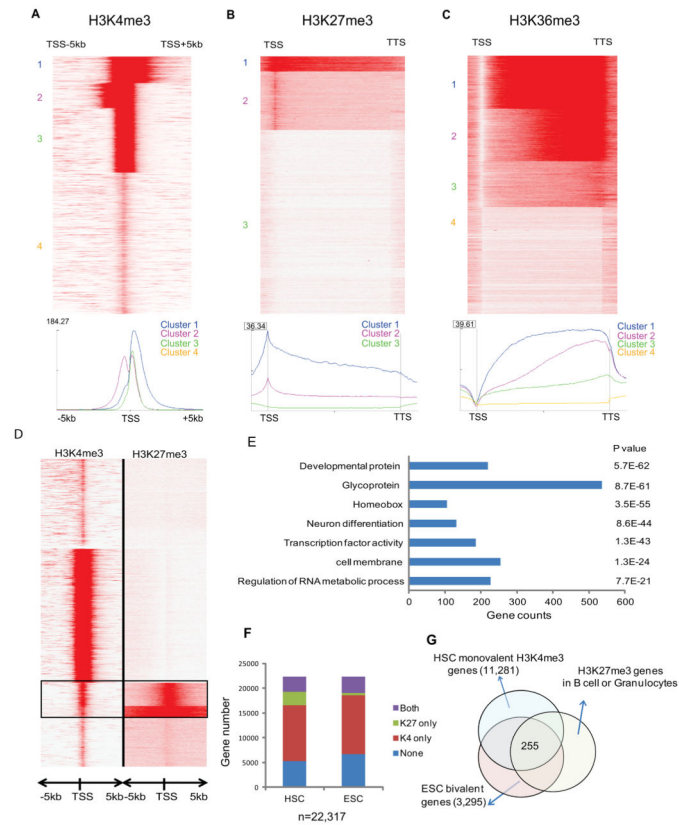


Figure 2. Histone marks in HSC

(A) Heatmap and profile of H3K4me3 around TSS of all Refseq genes. Red represents high intensity and White no signal; cluster IDs are marked to the left. The profile plot shows the average reads per region on the y-axis at each relative position to TSS on the x-axis, for the 3 clusters with H3K4me3 coverage.

(B) Heatmap and profile of H3K27me3 around the gene body of all Refseq genes. The profile plot shows the average reads per region on y-axis at each relative position on the x-axis, for the 3 clusters with H3K27me3 coverage. All genes are normalized to same length.

(C) Heatmap and profile of H3K36me3 around the gene body of all Refseq genes. The profile plot shows the average reads per region on y-axis at each relative position on the x-axis, for the 3 clusters with H3K36me3 coverage. All genes are normalized to same length.

(D) Unsupervised clustering of histone profiles around the TSS of the Refseq genes showed bivalent genes marked by both H3K4me3 and H3K27me3 in HSC.

(E) Gene ontology enrichment analysis for the bivalent genes in HSC. P values and gene counts are shown.

(F) The classification of Refseq genes according to co-binding patterns of H3K4me3 and H3K27me3 in HSC and ESC. “Both” represents H3K4me3 with H3K27me3.

(G) Venn diagram to show the HSC genes that share the listed chromatin modifications: bivalent in ESC, actively transcribed in HSC and repressed (H3K27me3) in differentiated B cell and Gr1 cells.

See also Figure S3

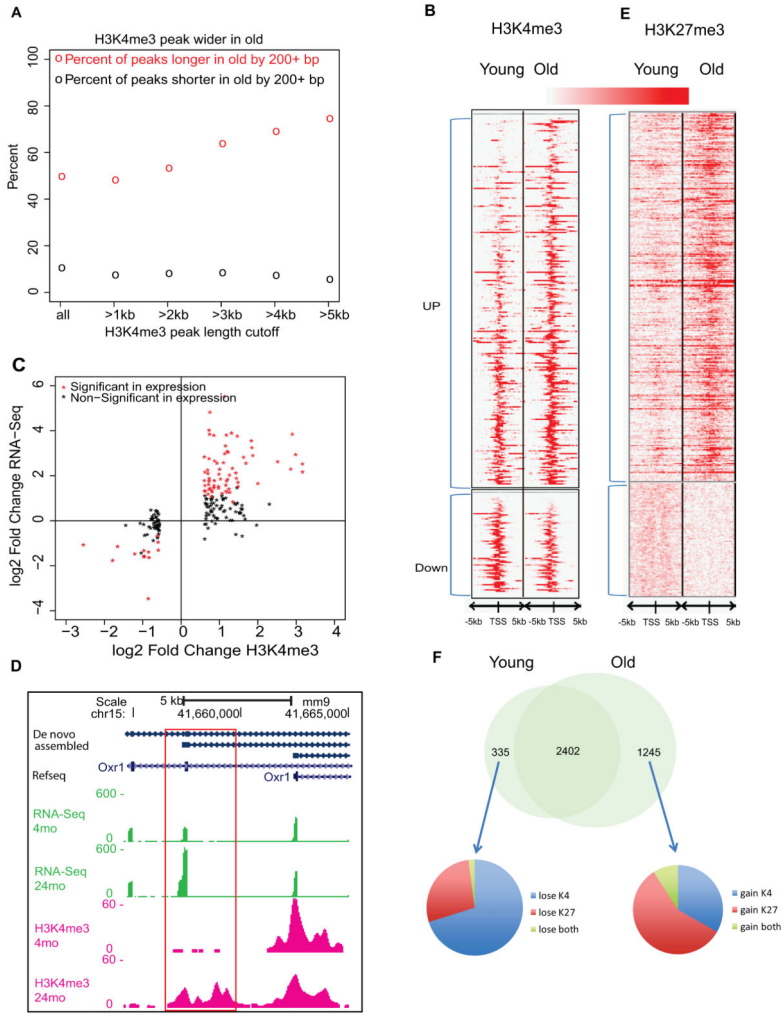


Figure 3. Histone modifications changes with HSC aging

(A) Percent of H3K4me3 peaks getting longer or shorter (>200bp) in old HSCs. The x-axis is the peak-length cutoff to be counted toward lengthening or shortening. The y-axis is the number of wider or shorter peaks divided by total number of peaks at the length cutoff. The circles represent the percent of lengthening (red) and shortening (black) events.

(B) Heatmap of H3K4me3 density around promoters that show significantly different H3K4me3 binding with age (Poisson P-value 10^{-8}).

(C) The correlation between gene expression and H3K4me3 signals for the significantly different H3K4me3 binding genes. The X-axis denotes the log₂ fold change of H3K4me3 ChIP-Seq read counts in the defined promoter region and the Y-axis denotes the log₂ fold change of FPKM value for the gene.

(D) Genome browser view on the *Oxr1* gene body. Boxed area shows new promoter with H3K4me3.

(E) Heatmap of H3K27me3 density around promoters that show significantly different H3K27me binding with age.

(F) Venn diagram showed bivalent domains change with HSC aging.

See also Figure S3

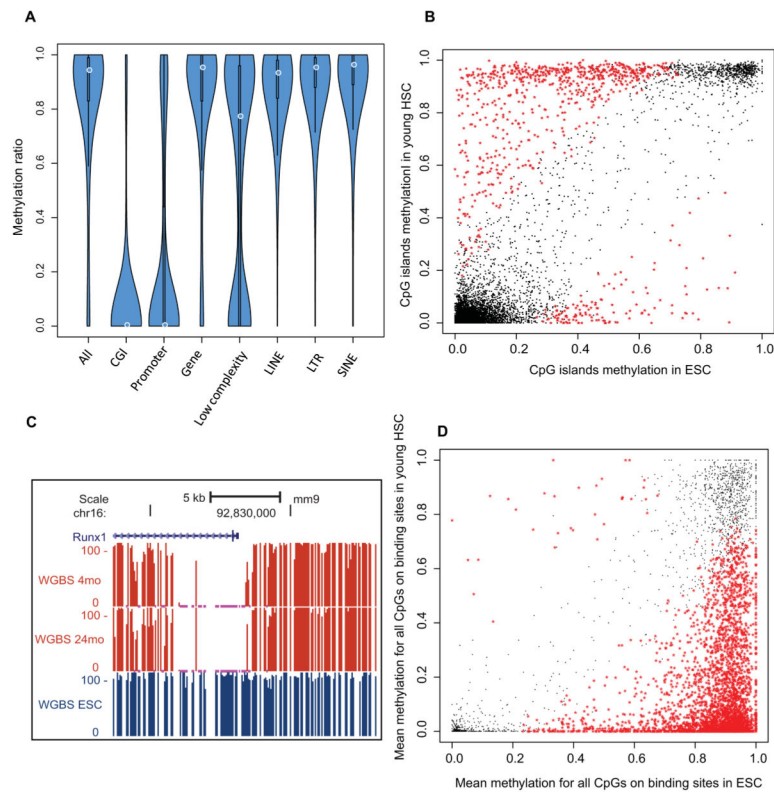


Figure 4. HSC specific methylome

(A) Violin plot showing DNA methylation ratios in different genomic features. The thickness of the bars indicates densities of CpGs at the y-axis ratio; the white circle indicates median.

(B) Scatter plot for mean methylation ratio for all the CpGs of each CGI in HSC compared with ESC. The x-axis and y-axis indicate the methylation ratio of each CpG island in HSC and ESC respectively. The black dots represent loci that are not significantly different between the cell types, and the red stars represent the CpG Islands that exhibit cell type-specific methylation.

(C) Genome browser view showing the percentage of methylation in the promoter of the *Runx1* gene in young and old HSCs and ES cells (ESC).

(D) Methylation ratios in HSCs versus ESC of *Runx1* binding sites as mapped in mouse HPC7 hematopoietic progenitor cells. Black and red as denoted in (B)

See also Figure S4

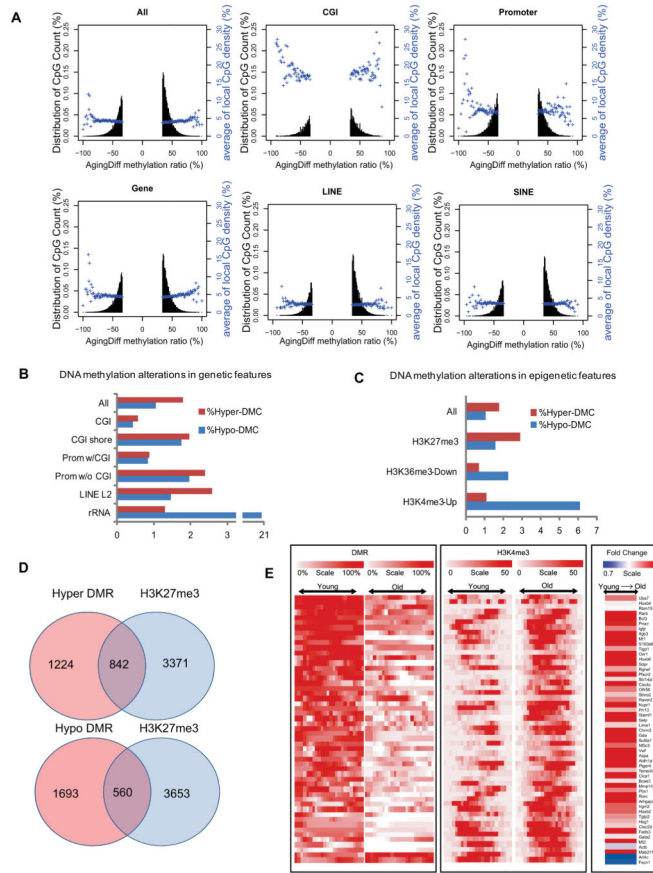


Figure 5. HSC methylome alterations with aging

(A) Plots show the degree of differential methylation in young versus old HSCs and the relationship between the local CpG density (blue). The top left plot shows all DMCs in old HSCs defined as CpGs that are 20% less methylated and 20% more methylated. The other plots show DMCs located within different genomic features.

(B) The percentage of hyper- (red) or hypo- (blue) DMCs in different genomic features.

(C) Interaction of DNA methylation and histone modifications. The percentage of DMCs in the indicated epigenetic features and their alterations with aging.

(D) Venn diagram showing the overlap of DMR genes with polycomb repressed genes in HSC.

(E) Heatmap of DNA methylation, H3K4me3 signal and expression values for 50 potential HSC aging markers. Each row represents a gene-associated region where there is coexistence of differential H3K4me3 and DNA methylation. For H3K4me3 and DNA methylation, the red color denotes high methylation and white denotes no methylation. For gene expression, red denotes up-regulation and white denotes down-regulation.

See also Figure S5

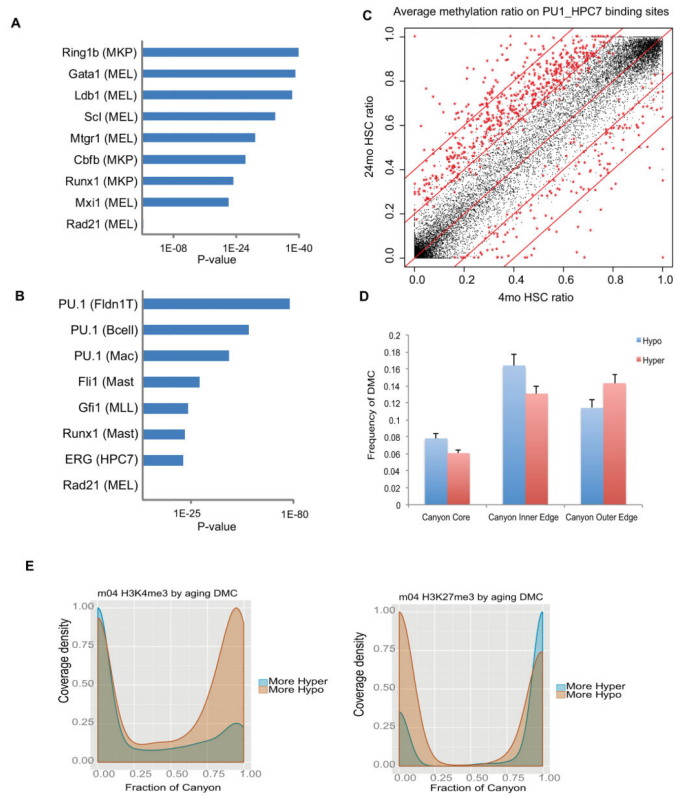


Figure 6. DNA methylation changes interact with transcriptional network

(A) Hypo-DMRs are enriched for the indicated transcription factor binding sites.

Parentheses () identify the cell type or cell line in which the TF binding sites were originally identified. MKP: Megakaryocyte progenitors; MEL: Murine erythroleukemia cell line.

(B) Hyper-DMRs are enriched for transcription factor binding sites in distinct blood lineages. Parentheses () identify the cell type or cell line in which the TF binding sites were originally identified. FLDN1_T: Fetal Liver DN1 T cell; Mac: Macrophage; Mast: Mast cells; MLL: MLL/ENL-expressing preleukemia cells; MEL: Murine erythroleukemia cell line.

(C) Scatter plot comparing the methylation ratio for all the Pu.1 binding sites identified in the HPC7 cell line between 4mo HSC and 24mo HSC. Red symbols indicate binding sites with methylation ratios significantly changed between 4mo HSC and 24mo HSC.

(D) Average number of CpGs in DNA methylation Canyon regions differentially methylated between 4mo and 24mo HSC. Canyons are defined in 12mo HSC. DMCs counts are normalized by region length. Canyon Core, region inset by 500 bp on each edge; Inner and Outer Edge, 500 bp regions inside and outside Canyon edges, respectively; Error bars, SEM.

(E) H3K27me3 (left) and H3K4me3 (right) peak coverage density of Canyons relative to aging DMCs. Density of peaks in 4mo HSC at Canyons subset by normalized counts of aging DMCs. H3K4me3 consists of H3K4me3 peaks alone. H3K27me3 consists of any peak region containing H3K27me3, including bivalent (co-occupancy by H3K4me3) and H3K27me3 alone. More Hypo and Hyper indicate Canyons with greater numbers of hypomethylated or hypermethylated DMCs, respectively.

See also Figures S6 and S7.

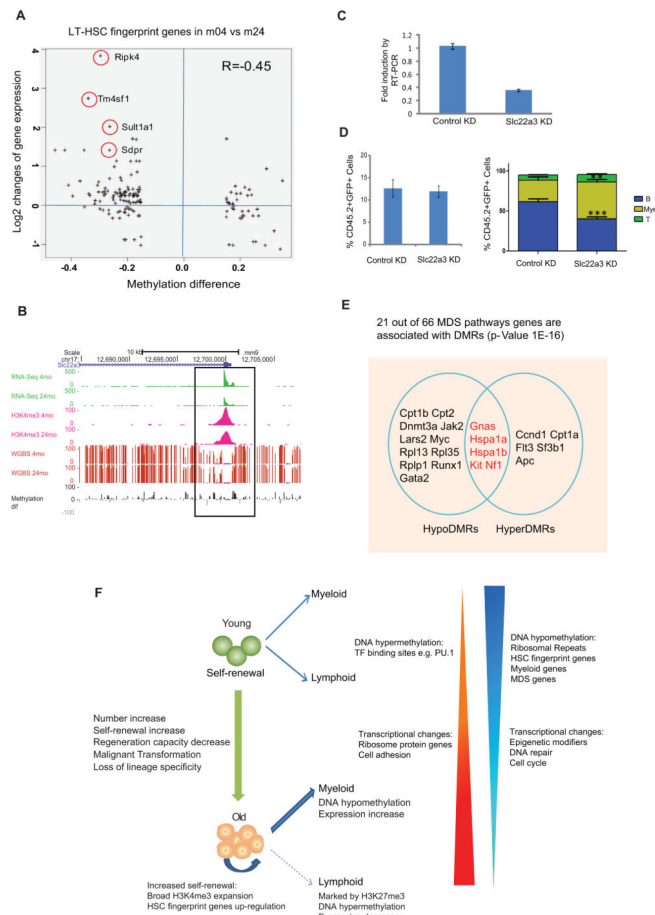


Figure 7. DNA methylation regulates HSC function and contributes to age-related diseases
 (A) The correlation between gene expression changes and methylation alterations for HSC fingerprint genes with DMR. The X-axis denotes the DMR methylation ratio difference, and the Y-axis denotes the log₂ fold change of FPKM value for the gene. The circles mark the gene with names aside.
 (B) UCSC browser track showing expression (green), DNA methylation (red bars), grey and black bars show differential methylation between 4m and 24m HSCs, H3K4me₃ signal (pink) for the TSS region of *Slc22a3* in young and old HSCs.
 (C) QRT-PCR to show that *Slc22a3* was knocked down by miRNA construct. Sca-1⁺ cells were enriched from 5-FU injected WT mice (4 month old) and transduced with retroviral miRNA construct. After in vitro culture for 2 days, 20,000 GFP⁺ cells were sorted for qRT-PCR.
 (D) Left figure showed the contribution of retrovirally-transduced donor HSCs (CD45.2⁺GFP⁺) to recipient mouse peripheral blood. Right figure showed the percentage of indicated lineages within the retrovirally-transduced donor HSC-derived (CD45.2⁺GFP⁺) cell compartment in peripheral blood post-transplant (8-weeks). Myeloid cells (Mye) were defined using the markers Gr1⁺ and Mac1⁺, B-cells (B) are B220⁺, T-cells (T) are CD4⁺ and CD8. n=8 for each group. *** P<0.001, ** P<0.01. Error bars represent Mean ± SEM.

(E) Venn diagram showing MDS genes with hyper or hypo-DMRs. Regions with overlap have both hyper- and hypo-DMRs within same gene (distinct regions).

(F) Model for functional and epigenetic alterations with HSC aging. DNA hypomethylation in ribosomal repeats could initiate chromosomal instability and indicate HSC activation state. DNA hyper- or hypo-methylation in master transcription factor binding sites could contribute to reinforcement of self-renewal program and inhibition of differentiation.